

Calibration of an Absolute Radiation Thermometer for Accurate Determination of Fixed-Point Temperatures

R. Winkler · E. R. Woolliams · W. S. Hartree ·
S. G. R. Salim · N. P. Fox · J. R. Mountford ·
Malcolm White · S. R. Montgomery

Published online: 11 October 2007
© Springer Science+Business Media, LLC 2007

Abstract For accurate determinations of thermodynamic temperature, NPL has developed its absolute radiation thermometer (ART), which is calibrated traceably against a cryogenic radiometer. This article reviews some of the potential sources of systematic uncertainty present in the calibration and use of ART. In particular, this article is concerned with the evaluation of the size-of-source effect and the lens transmittance, as well as potential differences in the responsivity of a transfer trap detector when calibrated in terms of radiant power and used in irradiance mode.

Keywords Filter radiometry · Lens transmittance · Radiation thermometry · Size-of-source effect · Thermodynamic temperature

1 Introduction

At high temperatures, a new addition to the *mise en pratique* for the kelvin is likely to allow the use of absolute radiometric methods for direct temperature measurement. For those without access to high accuracy radiometric calibration facilities, this will be mediated by high temperature fixed points, the temperature of which will be determined over the next few years as part of an international project organized by the CCT-WG5. Several national metrology institutes will be making definitive measurements of these fixed points using filter radiometry. In preparation for this, NPL in common with others is optimizing its filter radiometric facilities and calibration processes.

R. Winkler (✉) · E. R. Woolliams · W. S. Hartree · S. G. R. Salim · N. P. Fox · J. R. Mountford ·
M. White · S. R. Montgomery
Optical Technologies and Scientific Computing, DQL, National Physical Laboratory, Hampton Rd,
Teddington, Middlesex, TW11 0LW, UK
e-mail: rainer.winkler@npl.co.uk

2 Filter Radiometry

Absolute filter radiometry is based on the determination of the radiance of a blackbody source within a narrow wavelength range. From this measurement, and Planck's law, the temperature of the blackbody source can be determined directly. Spectral radiance requires a measurement of power (achieved by traceability to the cryogenic radiometer) within a defined solid angle (achieved by a geometric system traceable to the meter) and within a defined spectral band (achieved by a bandpass filter and traceable to the meter via the wavelength of a tuneable laser).

At NPL, spectral radiance is measured using the absolute radiation thermometer (ART), a very simple device consisting of a linear arrangement of a 75 mm diameter plano-convex silica lens, a 40 mm diameter thin film aperture directly behind the lens, and a filter radiometer (as described in [1]) at a distance of 2,100 mm from the lens. The filter radiometer has a peak wavelength of 800 nm and a bandwidth of 20 nm. It is fitted with a 5 mm diameter brass aperture and a black-anodized cover. All optical elements are embedded in an Invar frame and covered by a common enclosure. To reduce stray light, all mechanical elements are blackened and two baffles have been added. The filter radiometer is temperature stabilized to $\pm 0.02^\circ\text{C}$ to minimize any effects due to temperature sensitivity of the spectral filter.

A three-element reflection trap [1] is used to transfer the spectral responsivity calibration from a cryogenic radiometer to the ART filter radiometer. The trap is calibrated at a few wavelengths in the region of interest, using a laser beam that underfills the detector, and its responsivity (in $\text{A} \cdot \text{W}^{-1}$) is interpolated between these wavelengths [1]. A calibrated diamond-turned brass aperture of the same nominal diameter as that of the filter radiometer is then added to the trap for the filter radiometer calibration, which requires the detectors to be overfilled as for the filter radiometer measurement. The spectral responsivity of the filter radiometer (in $\text{A} \cdot \text{W}^{-1} \cdot \text{m}^{-2}$) is then determined with this trap detector and an integrating sphere illuminated by a Ti:Sapphire laser, tunable over the band-pass region of the filter radiometer [7]. The geometric system is defined by the lens aperture area and the distance between the filter radiometer aperture and the lens aperture as determined with interferometer-based measurement systems. Through this mechanism, the spectral radiance measurements are traceable to the cryogenic radiometer.

This would be sufficient for a theoretically perfect system, but for a real system, an absolute temperature measurement requires correction for the lens transmittance and the size-of-source effect (SSE) of the instrument (see, e.g., [2] for a general introduction to the concept).

In order to achieve the lowest uncertainties, the SSE and lens transmittance, and the addition of an aperture to the trap detector, needed to be fully evaluated. The simple design of ART allowed us to look at the SSE and lens transmittance through two routes:

- (i) both as separate entities, that can be combined, and
- (ii) in a single measurement.

These “in parts” and “as a whole” calibrations can then be compared, giving confidence that all systematic sources of uncertainty had been considered.

3 Determining the Size-of-Source Effect

An absolute determination of radiance requires the determination of the ratio of the light collected with the non-ideal instrument from a (real) blackbody source to the light that would be collected with (a) the instrument free of the size-of-source effect or (b) an infinitely large uniform temperature blackbody source.

Previously, it was assumed that the SSE curve asymptotically approaches a finite value for large (but experimentally accessible) source diameters and that the SSE value for a sufficiently large source diameter can approximate the value for an infinite source diameter [2]. Although this is a reasonable assumption, it is nevertheless a potential source of uncertainty, since one cannot be entirely sure what happens to the SSE between a finite and an infinite source diameter. Such considerations and the observation that their instrument's SSE kept increasing, even at large source diameters, led Goebel et al. [3] to devise an experiment capable of revealing such a systematic effect. They determined the SSE and the lens transmittance first in two separate experiments and then in one 'combined' measurement. This experiment was repeated for ART in an adapted form.

In recent years, doubts have not only been raised about the equivalence of the SSE at a 'sufficiently large diameter' and an infinite diameter, but concerns were also voiced about the determination of the SSE even at experimentally accessible diameters. Generally, two different methods are employed for the determination of the size-of-source effect: the 'direct' and the 'indirect' techniques. Although traditionally thought to be equivalent, it has been reported that they can give different results, especially at larger diameters [4]. In this article, we present a further comparison of the methods and an alternative implementation of the direct technique.

The results of these SSE measurements are then combined with a lens transmittance measurement and compared to the results of a combined lens transmittance and SSE measurement.

3.1 SSE Measurements

ART's design is very simple, which facilitates the study of systematic effects, since all the optical elements within ART are easily exchangeable. However, the simplicity gained by omitting the additional optics suggested by Yoon et al. [5] comes at the cost of a larger size-of-source effect. Two baffles were introduced into ART after a systematic experimental study of internal stray-light effects, and these improve the SSE behavior, especially at larger diameters.

3.1.1 SSE—The Indirect Technique

The indirect measurement employed an integrating sphere illuminated by a tungsten halogen light source with a Perspex plate fitted to its exit aperture. This front plate contains a central obscuration in the form of a 2.5 mm diameter miniature blackbody cavity. Different sized apertures can be attached directly to the front of the plate. The apparatus and the measurement procedure are described in more detail in [4] and [6].

The sphere is placed such that the surface of the Perspex plate sits in the object plane of the radiation thermometer.

The level of back reflection of light into the sphere was, however, dependent on the aperture size. To evaluate this, a photodiode was mounted at one of the side ports of the sphere. Its signal changed by 0.83% from the smallest to the largest aperture. This effect was found to influence the result of the measurement by $< 0.002\%$.

3.1.2 SSE—*The Direct Technique*

The setup for the direct technique consisted of a variable iris aperture in the object plane of ART illuminated by an integrating sphere. The SpectralonTM-coated sphere had an inner diameter of approximately 300 mm and a front port of 106 mm diameter. Laser radiation from a tuneable Ti:sapphire laser set to a wavelength corresponding to the peak response of ART (i.e., 800 nm) was fed into the sphere via an optical fiber. The laser radiation was de-speckled with the help of an ultrasonic water bath in order to provide a uniform and stable radiation field [7]. On another side port, the sphere was fitted with a silicon photodiode, which provided the feedback signal for the power stabilization of the laser.

For the measurements, the iris was set to a large diameter after each reading of the ART's response to a specific source diameter. This reference signal accounted for any short-term changes in the laser output. A measurement of the dark signal was made (by covering the iris) before and after each set of measurements. It was found to have no significant effect on the results. The laboratory lights were switched off for the duration of the experiment in order to minimize the effect on the feedback signal for the laser stabilization.

When the integrating sphere was placed directly behind the iris, the experiment gave inconsistent and implausible results: the signal of the filter radiometer changed by up to 20% when the iris was opened from a diameter of 3–20 mm. This is likely caused by light that is directly back-reflected from the iris onto the monitoring photodiode, thereby biasing the feedback signal.

The sphere was moved back by 250 mm to avoid problems of this nature. In order to evaluate whether there were still any remaining inter-reflections, the sphere was moved further back to a position of 920 mm behind the iris. In this position, the integrating sphere could only illuminate the object plane of ART to a diameter of 19 mm. The differences between the SSE measurements performed with these two setups are shown in Fig. 1. The fact that these two measurements agree very well indicates that there are no further significant stray light/inter-reflection problems.

3.1.3 SSE—*Comparison of the Direct and Indirect Techniques, Results*

Blackbodies measured by ART typically have an inner crucible diameter of 3 mm. Therefore, the SSE measurements were performed from this diameter upward. Figure 2 shows that the results of the direct and the indirect techniques agree very well, except for the very small and very large diameters. The differences between diameters of 3 and 4 mm are irrelevant for an overall SSE correction since the radiance profiles of the blackbodies are very close to unity in this region. At 50 mm diameter, the

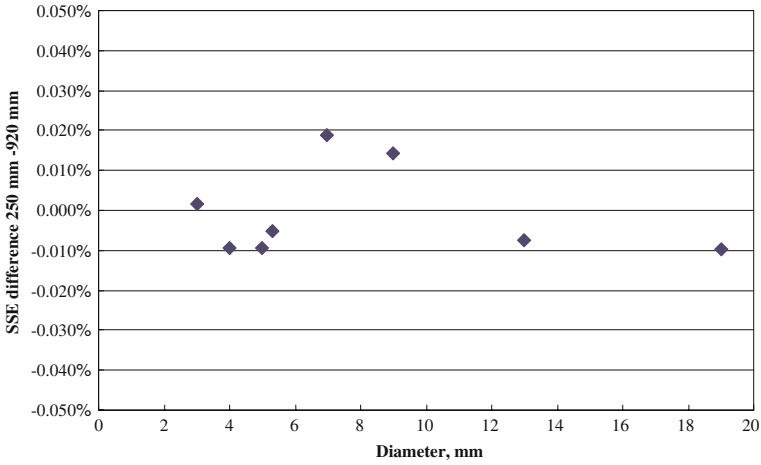


Fig. 1 SSE with integrating sphere at 250 and 920 mm behind iris

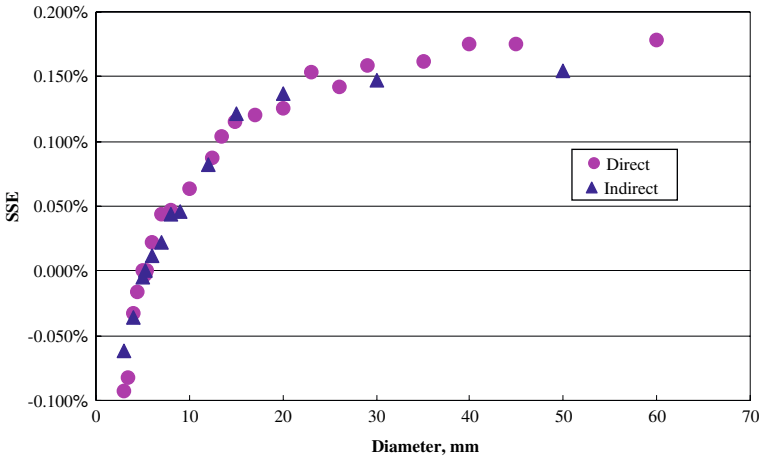


Fig. 2 SSE with direct and indirect techniques

indirect method gives a value that is 0.026% lower than that of the direct method. The significance of this difference will be discussed below.

4 Lens Transmittance and SSE

4.1 Lens Transmittance and SSE—Combined Measurement

Figure 3 shows the setup for this measurement. In the ‘radiance mode,’ a 5.3 mm diameter aperture is placed in the object plane of ART and the signal V_{rad} is obtained. In the ‘irradiance mode,’ the lens is removed from ART, the 5.3 mm aperture is removed from the object plane of ART, and the signal V_{irrad} is measured.

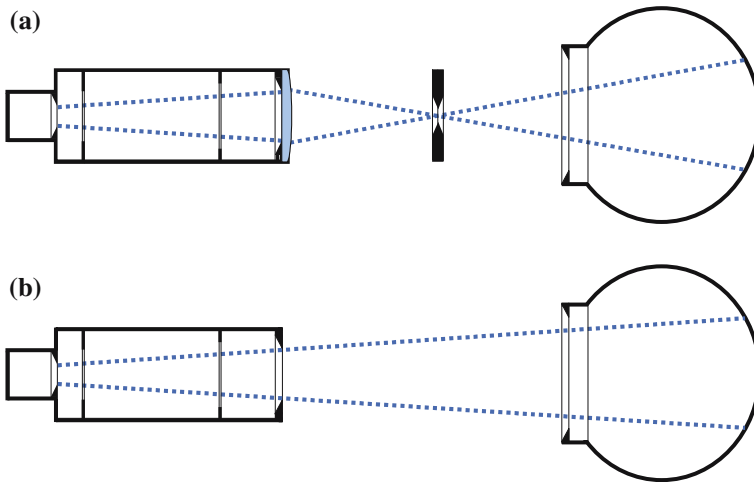


Fig. 3 Combined lens transmittance/SSE experiment: (a) ‘radiance mode’ and (b) ‘irradiance mode’

V_{irrad} was corrected for diffraction effects. This corrected signal represents the signal ART should measure if its lens were transmitting light perfectly and if it were not suffering from the SSE. The diffraction correction is close to unity, since the integrating sphere aperture is significantly larger than the source diameter of approximately 70 mm that is required to illuminate the system entirely. The diffraction correction F_{diff} was calculated using two different methods via Focke’s and Wolf’s algorithm as implemented by Edwards [8,9]. Both methods gave the same value of $F_{\text{diff}} = 0.99978$ to five significant places.

The same integrating sphere that was also used for the direct SSE measurement was placed such that both setups were irradiated by light originating from the same part of the sphere, which was calculated to be approximately 1,600 mm from the ART’s lens aperture. This was to avoid any problems that might be caused by non-uniformity of the sphere. The sensitivity of the measurement to the positioning of the sphere was evaluated by moving the sphere over a distance of 200 mm along the optical axis (the end position was 1,800 mm). This was done separately in the ‘radiance’ and ‘irradiance modes,’ and was repeated several times. The deviation of each signal from the average with respect to the displacement of the sphere is shown in Fig. 4. Both signals decreased in a linear fashion and at the same rate of approximately 0.02% per 100 mm. Their ratio was therefore independent of the exact positioning of the sphere.

The ratio between the radiance mode signal and the diffraction-corrected irradiance mode signal is the correction factor necessary to calibrate ART as a whole against a source of known radiance and of known finite size. For a source diameter of 5.3 mm, this correction factor C_{cal} was found to be equal to

$$C_{\text{cal}} = \frac{1}{F_{\text{diff}}} \times \frac{V_{\text{rad}}}{V_{\text{irrad}}} = \frac{1}{0.99978} \times 0.93014 = 0.93034 \quad (1)$$

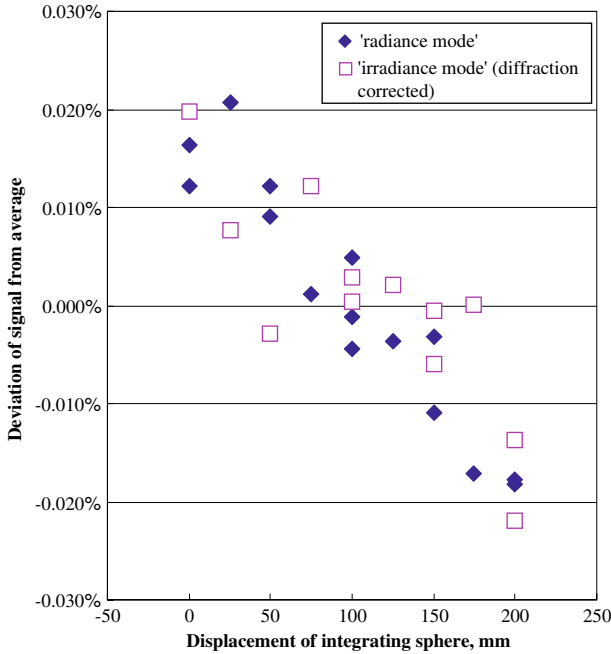


Fig. 4 Influence of the sphere position

4.2 Lens Transmittance and SSE—Measurement in Parts

The transmittance τ of ART’s lens was measured at 800 nm using an experiment arrangement as described in [10]. Its value was found to be $\tau = 0.93203$, with an associated uncertainty less than 0.01%.

Assuming that the SSE value at 60 mm diameter as determined by the direct method is a good approximation to the value at an infinite source diameter, the correction factor C_{cal} is

$$C_{cal} = \tau \times \frac{\int_0^{d_{ref}} \frac{\partial \sigma(x)}{\partial x} dx}{\int_0^{d_{\infty}} \frac{\partial \sigma(x)}{\partial x} dx} = 0.93203 \times \frac{1}{1.00181} = 0.93035, \tag{2}$$

where $\sigma(x)$ is the normalized signal of ART to a uniform source of diameter x such that $\sigma(d_{ref}) = 1$.

This is very close to the value calculated for the calibration ‘as a whole.’

If the indirect method is used to calculate the same correction factor C_{cal} , the result is 0.93059, with an associated uncertainty less than 0.01%.

4.3 Comparison of the Two Approaches and Overall Correction

The correction factor discussed so far is appropriate for a first comparison of the methods, but the correction that is of interest in temperature measurements must take into account the blackbody radiance profile, C_{BB} :

$$C_{BB} = \frac{\int_0^{d_{BB}} \frac{\partial \sigma(x)}{\partial x} \rho(x) dx}{\int_0^{d_{ref}} \frac{\partial \sigma(x)}{\partial x} dx}, \tag{3}$$

where $\rho(x)$ is the normalized radiance of the blackbody at diameter x such that $\rho(0) = 1$ and d_{BB} is the diameter up to which the blackbody is emitting significant radiation.

For a more intuitive understanding, C_{BB} can also be shown to be equal to

$$C_{BB} = 1 + \frac{\int_0^{d_{BB}} \frac{\partial \sigma(x)}{\partial x} \rho(x) dx - \int_0^{d_{ref}} \frac{\partial \sigma(x)}{\partial x} [1 - \rho(x)] dx}{\int_0^{d_{ref}} \frac{\partial \sigma(x)}{\partial x} dx}. \tag{4}$$

This equation illustrates that the measurement of the true shape of the SSE curve is least critical for the determination of C_{BB} (a) the closer $\rho(x)$ is to unity for diameters smaller than d_{ref} and (b) the closer $\rho(x)$ is to zero for diameters greater than d_{ref} .

The correction factor that includes all corrections for SSE and lens transmittance is $C_{overall}$:

$$C_{overall} = C_{cal} C_{BB}. \tag{5}$$

Table 1 shows the overall correction factors $C_{overall}$ for the SSE and lens transmittance after the radiance profile of a Re-C blackbody has also been taken into account.

Three of the values are within a range of 0.006%. One of the values is 0.022% higher than the average of the other three. This reflects the difference in the direct and indirect

Table 1 Results of the different SSE/lens transmittance experiments

Calibration as a whole		Calibration in parts	
Direct SSE technique	Indirect SSE technique	Direct SSE technique	Indirect SSE technique
0.93128	0.93125	0.93131	0.93150
Average=0.93134			
SEOM=0.00007			
Semi range/ $\sqrt{3}$ = 0.00007 (assuming rectangular distribution)			

SSE determinations at larger diameters, especially since there is no significant black-body radiation beyond 30 mm diameter. The results for the ‘calibration as a whole’ are very close, independent of which SSE determination is used. This is because the blackbody radiance profile is close to unity for smaller diameters ($\rho(x) > 0.87$, for all diameters $x < 5.3$ mm diameter).

5 Addition of an Aperture to the Transfer Trap

The three-element trap (basic design as in [11]) is calibrated against the cryogenic radiometer using a collimated laser beam of approximately \varnothing 3 mm. At this stage, it is not fitted with an aperture.

However, when the trap is used for the calibration of the filter radiometer, a brass aperture is added. In this step of the calibration chain, the trap aperture is overfilled with a diverging beam ($f/52.5$). It is important to consider whether internal reflections can contribute significantly to the signal. Considering first the specular reflections: the light undergoes five reflections within the trap, returning of the order of 0.4% of the incoming flux at 800 nm [11] toward the aperture, approximately a third of which hits the back metal side of the aperture. The aperture is angled so that this light is reflected into the aluminum housing of the trap. Even in the worst-case scenario, assuming that all of the light undergoes only these two reflections before hitting a photodiode, one would be left with a contribution to the main signal of a few parts in 10^4 . Since most of the light will undergo multiple reflections before reaching a photodiode, it is reasonable to assume that the effect of specular reflections will be insignificant at the 10^{-4} -uncertainty level. However, it has been suggested [12] that a high level of diffuse reflection might be present inside the trap detector. This would complicate matters far beyond the limits of a simple theoretical deduction.

For these reasons, one of the NPL three-element traps was experimentally compared to a TKK (Helsinki University of Technology) six-element transmission trap (basic design as described in [13] and [14]) when varying the beam geometry from quasi-collimated ($f/430$) to $f/38$. The designs of the two traps are sufficiently different, so that, if there were a significant effect due to the presence of an aperture, one would expect that this effect would be recognizably different for the two traps. When changing the f -number of the incoming beam, the ratio between the trap signals should therefore change significantly.

During the time of these experiments, the version of ART as described in the introduction was used for eutectic measurements [15]. A previous and slightly shorter version of ART that is yet similar in all other respects was used for the measurements reported here. The static filter radiometer mount was removed in order to place a computer-controlled stage with several detector mounts behind this version of ART. A three-element reflection trap was attached to one of the mounts and the six-element transmission trap to another. Both traps were fitted with nominal 5 mm diameter apertures and were set to a distance of 1,720 mm behind the lens. The lens was held in place with a 60 mm diameter aperture (instead of the 40 mm diameter aperture) and was fitted at the front with a variable iris. A small integrating sphere was placed in the object plane and fed with light of wavelength 752 nm from a stabilized laser-source. The iris

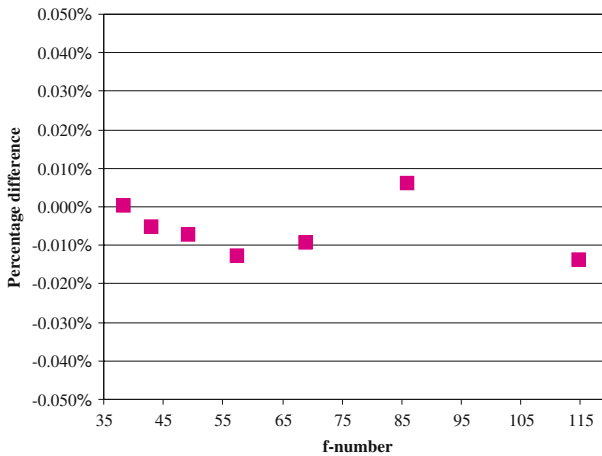


Fig. 5 Differences in trap ratios depending on the f-number of the irradiating beam

was set to a diameter of 4 mm, and the trap detectors were subsequently exposed to the radiation field in the image plane of the setup. Then, the ratio of these dark-corrected trap signals was calculated. Following that, the iris was set to diameters of 15 mm (f/115) to 45 mm (f/38) in steps of 5 mm. At each of these settings, the same ratio was calculated and the difference to the ratio at 4 mm diameter is shown in Fig. 5. This indicates that there is no significant effect due to specular or diffuse reflections at the 10^{-4} -uncertainty level.

6 Conclusions

These investigations show that the standard uncertainty due to the SSE correction is less than 0.01% and that there is no significant effect due to adding an aperture to the transfer trap detector.

This thorough evaluation has provided NPL with increased confidence in the reliability and robustness of its absolute filter radiometric methods and the traceability of the ART radiometer. This has allowed us to perform some early measurements of four eutectic cells [15] with high accuracy and would provide useful evidence in support of the planned CCT measurement campaign [16].

Future work will involve the use of these techniques to evaluate other radiation thermometers including those, which have been designed specifically to have relatively low SSE.

Acknowledgments The authors would like to thank their colleague Dave Lowe who provided the SSE facility for the indirect measurement and gave advice on how to operate it. This work was supported by the National Measurement System Policy Unit of the UK Department of Trade and Industry.

References

1. V.E. Anderson, N.P. Fox, *Metrologia* **28**, 135 (1991)
2. N.P. Fox, J.E. Martin, D.H. Nettleton, *Metrologia* **28**, 357 (1991)
3. R. Goebel, Y. Yamada, M. Stock, in *Proceedings of TEMPMEKO 2004, 9th International Symposium on Temperature and Thermal Measurements in Industry and Science* (FSB/LPM, Zagreb, Croatia, 2004), pp. 91–99
4. G. Machin, R. Sergienko, in *Proceedings of TEMPMEKO 2001, 8th International Symposium on Temperature and Thermal Measurements in Industry and Science* (VDE Verlag, Berlin, 2002), pp. 155–160
5. H.W. Yoon, in *Proceedings of TEMPMEKO 2004, 9th International Symposium on Temperature and Thermal Measurements in Industry and Science* (FSB/LPM, Zagreb, Croatia, 2004), pp. 521–526
6. D. Lowe, M. Battuello, G. Machin, F. Girard, in *Temperature: Its Measurement and Control in Science and Industry*, vol. 7, Part 2, ed. by D.C. Ripple (AIP Conference Proceedings, Chicago, 2002), pp. 625–630
7. V.E. Anderson, N.P. Fox, D.H. Nettleton, *Appl. Opt.* **31**, 536 (1992)
8. P.J. Edwards, *Diffraction Theory and Radiometry* (Ph.D. Dissertation, University of London, 2004)
9. P. Edwards, M. McCall, *Appl. Opt.* **42**, 5024 (2003)
10. E.R. Woolliams, D.P. Pollard, N.J. Harrison, E. Theocharous, N.P. Fox, *Metrologia* **37**, 603 (2000)
11. N.P. Fox, *Metrologia* **28**, 197 (1991)
12. E. Ikonen, Personal communication (2006)
13. J.L. Gardner, *Appl. Opt.* **33**, 5914 (1994)
14. T. Kübarsepp, P. Kärhä, E. Ikonen, *Appl. Opt.* **36**, 2807 (1997)
15. S.G.R. Salim, N.P. Fox, E.R. Woolliams, R. Winkler, D.H. Lowe, G. Machin, T. Sun, K.T.V. Grattan, Absolute Determination of the Thermodynamic Temperature of Four Eutectic Fixed Points. in *Proceedings of TEMPMEKO 2007* (to be published in *Int. J. Thermophys.*)
16. G. Machin, Y. Yamada, P. Bloembergen, M(C)-C eutectic research plan—the next steps, <http://www.bipm.fr/wg/AllowedDocuments.jsp?wg=CCT-WG5> Accessed 1 Feb 2007